J. Univ. Kuwait (Sci.) **11**, 1984

Effect of end restraint in triaxial testing of crushed rock

MOSAID AL-HUSSAINI

Department of Civil Engineering, University of Kuwait

ABSTRACT

Tests were carried out on crushed Napa basalt in a triaxial compression apparatus to examine the influence of the boundary restraint and the methods of consolidation on the observed stress–strain behaviour. Conventional as well as enlarged low-friction end platens were used in the test program. The K_0 consolidation tests were conducted, using a special lateral strain sensor. The specimens were prepared at two initial relative densities (70 and 100%) and sheared under drained conditions at consolidation pressures of 413, 861, 2067 and 3445 KN/m^2.

The results show that, for the material tested, the effect of low end restraint is to increase both the uniformity of radial strain on the boundaries and the axial strain at failure. The use of lubricated low-friction platens in triaxial testing has no significant effect on volume change but reduces the effective angle of internal friction in comparison with conventional triaxial testing.

INTRODUCTION

Understanding the mechanical properties of soil requires tests in which the principal stresses and strains can be determined at any section of a deformed specimen. This requirement is not always satisfied by the current testing techniques because the boundary conditions imposed on the specimen by simple mechanical means create a stress condition of undetermined magnitude.

The stress and strain distribution in a test specimen is influenced by several factors such as the density distribution of the material, the boundary conditions imposed by the end platens, and the flexible rubber membrane surrounding the specimen. These testing variables have an unknown effect on the average measured stresses and strains needed for strength calculations.

Of these testing variables, density non-uniformity can be minimised by the presently available technique of sampling and specimen preparation. Also, the rubber membranes are manufactured with uniform strength and flexibility which can be accounted for. Thus, the most likely factor which induces non-uniformity throughout soil specimens in triaxial testing is mainly related to restraints imposed by the rigid top and bottom platens.

LITERATURE REVIEW

The effect of end restraint on triaxial compression test results has been studied both analytically and experimentally by several investigators. From the analytical point of view, Filon (1962) appears to be the first to provide a closed-form solution for the stress distribution in a uniaxial compression elastic specimen with fixed ends. Since then, several elastic solutions were proposed (Pickett 1944; Balla 1960; Brady 1971a; Peng 1971), each being based on a different assumption to represent the frictional resistance between the specimen and the platens. Because of the different assumptions used in representing the end restraints, the resulting closed-form solutions differ slightly. For non-linear materials or complicated boundary conditions, these solutions may serve to provide the general trends of stresses and deformations within a test specimen.

The advent of high speed computers coupled with the finite element method made it possible to investigate the influence of specimen end conditions on the stresses and deformations in triaxial testing. Probably the first numerical solution to the problem of end restraint in an elastic cylinder under uniaxial compression was presented by D'Appolonia & Newmark (1951), who utilized the Lattice Analogy Technique. Since then, several finite element solutions for the problem of end restraint in an elastic cylinder under uniaxial compression have been published (Perloff & Pombo 1969; Girijavallabhan 1970; Brady 1971b). These analyses showed that the stress distribution for the same degree of end restraint is a function of Poisson's ratio as well as the height:diameter ratio of the specimen. A comprehensive finite element analysis was used to study the influence of end restraint on the stress distribution in a triaxial compression specimen with non-linear behaviour (Radhakrishnan 1972), The variation of the vertical stresses σ_z and the shear stress τ_{rz} at the top of the triaxial specimen as obtained from the closed-form solution (Pickett 1944; Balla 1960) and from the numerical procedures (D'Appolonia & Newmark 1951; Girijavallabhan 1970; Radhakrishnan 1972) along the radial distance of the specimen, with a height:diameter ratio of 1, are shown in Fig. 1. The variation of the shear stress, τ_{rz}, and vertical stress σ_z within an elastic cylinder, with a height:diameter ratio of 2, fixed at the end and subjected to uniaxial compression are shown in Fig. 2. This figure indicates that the vertical and shear stresses are the least uniform in the upper and lower sixth of the specimen of the triaxial specimen. The highest concentration of stresses occurs at the upper corner due to the greatest confinement effect. A similar trend was also indicated by previous investigators (Girijavallabhan & Mehta 1969; Radhakrishnan 1972; Lee 1978).

In experimental soil mechanics it is commonly assumed that stresses and strains are uniformly distributed within the triaxial specimens and they are consequently computed on the average dimensions of the entire specimens. An experimental study (Shockley & Ahlvin 1960) on a large triaxial specimen showed that there is a significant variation of stresses in the axial and radial directions, attributed to the end restraints. One of the earliest methods of eliminating the end restraint effects (Cooling & Golder 1940) uses a cone shaped platen in order to make the specimen preserve its cylindrical shape during shear. A more effective method (Rowe & Barden 1964) is to use a silicon–grease–rubber cushion between the soil and the platens. This method allows the use of a specimen with a length:diameter ratio of 1 (rather than 2 or more as used in a conventional triaxial test). The procedure of reducing end restraint by greased rubber cushion was used by various investigators (Rowe & Barden 1964; Bishop & Green

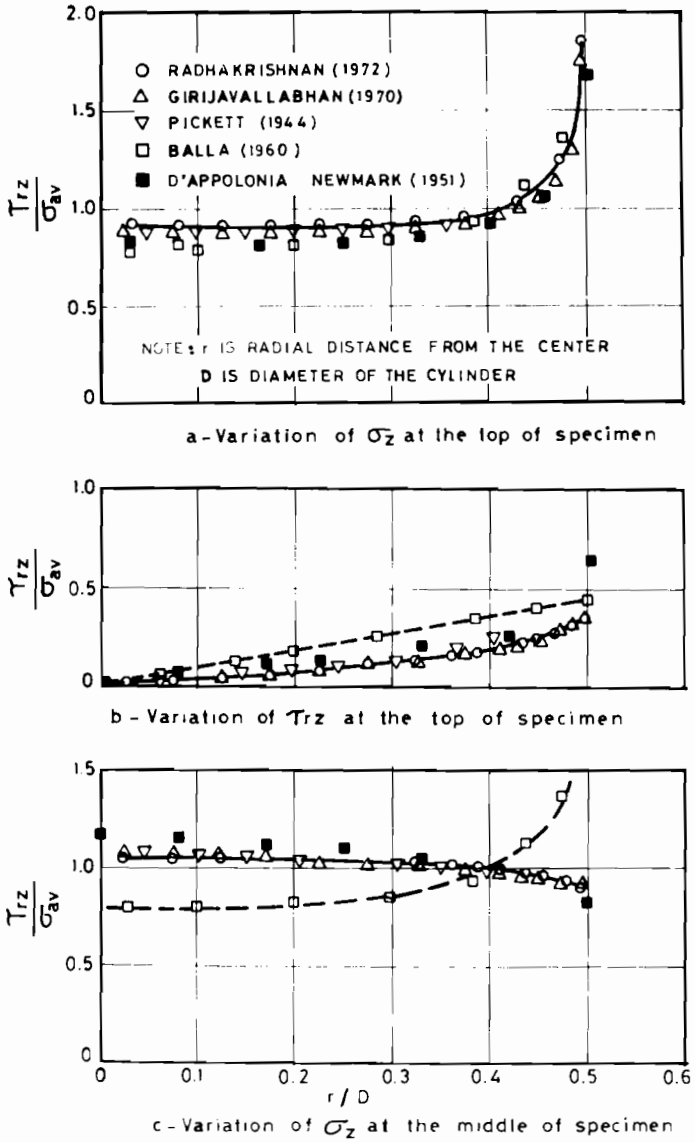

Fig. 1. Variation of σ_z and τ_{rz} at the top of the triaxial specimen with a height:diameter ratio of 1.

1965; Barden & McDermott 1965; Duncan & Dunlop 1968; Al-Hussaini 1970, Lee 1978; Norris 1981) on different types of soil but provided some conflicting conclusions with respect to the results obtained and the usefulness of the approach in comparison to the conventional triaxial testing method.

From the preceding survey of a limited number of theoretical and experimental studies performed previously, one may conclude that the elimination of end restraint effects reduces stress concentration and creates a more uniform strain distribution throughout the triaxial specimen, thus allowing the use of shorter specimens. The use of lubricated end platens in triaxial testing generally causes the specimen to exhibit a

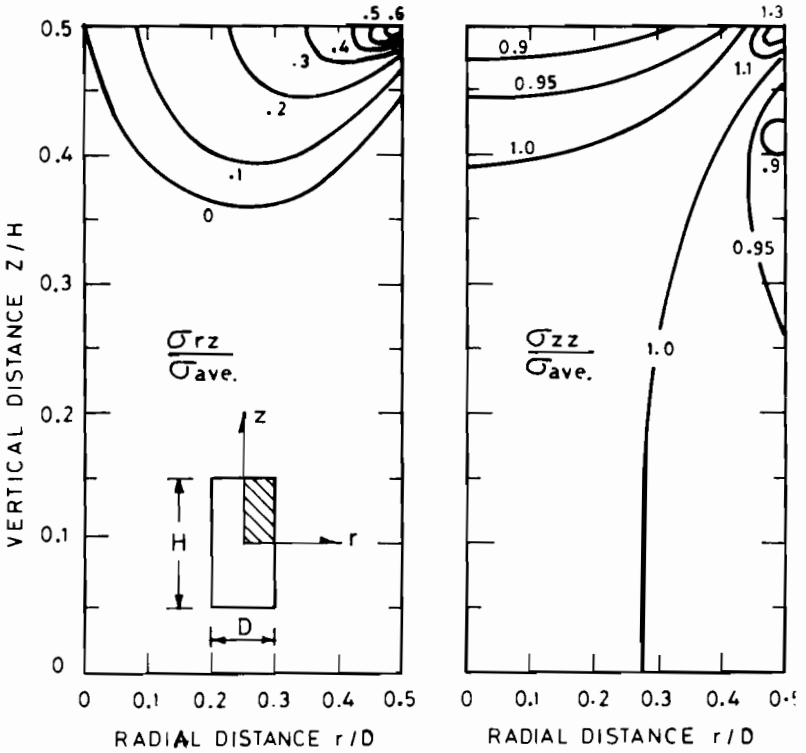

Fig. 2. Variation of σ_z and τ_{rz} in the triaxial specimen with a height:diameter ratio of 2.

lower tangent modulus, somewhat less strength, and a higher tendency to dilate as compared to using regular platens. The use of lubricated end platens, however, requires a more complicated test set-up and may cause the specimen to slide during shear. Most of the previous experimental studies were conducted on clays or fine sand. To the writer's knowledge there is no prior study pertaining to the effect of end restraints on the drained compression test of a crushed material at a wide range of confining pressure values.

EFFECT OF PLATEN MATERIAL ON END RESTRAINT

To eliminate the frictional resistance between the platen and the soil in a compression test might not generally be practical or easy. It has been suggested, however (Rowe & Barden 1964), that if the angle of friction between the platen and the soil is less than one degree, then the effect of the end platen can be considered negligible. In order to select the plate materials for use in this study, several direct shear tests were performed with the lower part of the shear device replaced by smooth surfaces of brass, aluminium, lucite and stainless steel blocks, and the results are presented in Fig. 3. These indicate that polished stainless steel offers the least frictional resistance, with or without greased cushions, in comparison to the other materials used for platens. The angle of friction between the polished steel and the crushed rock was about 8·9°, which dropped to 1·8°, when a lubricated rubber membrane was used to separate the soil from the stainless

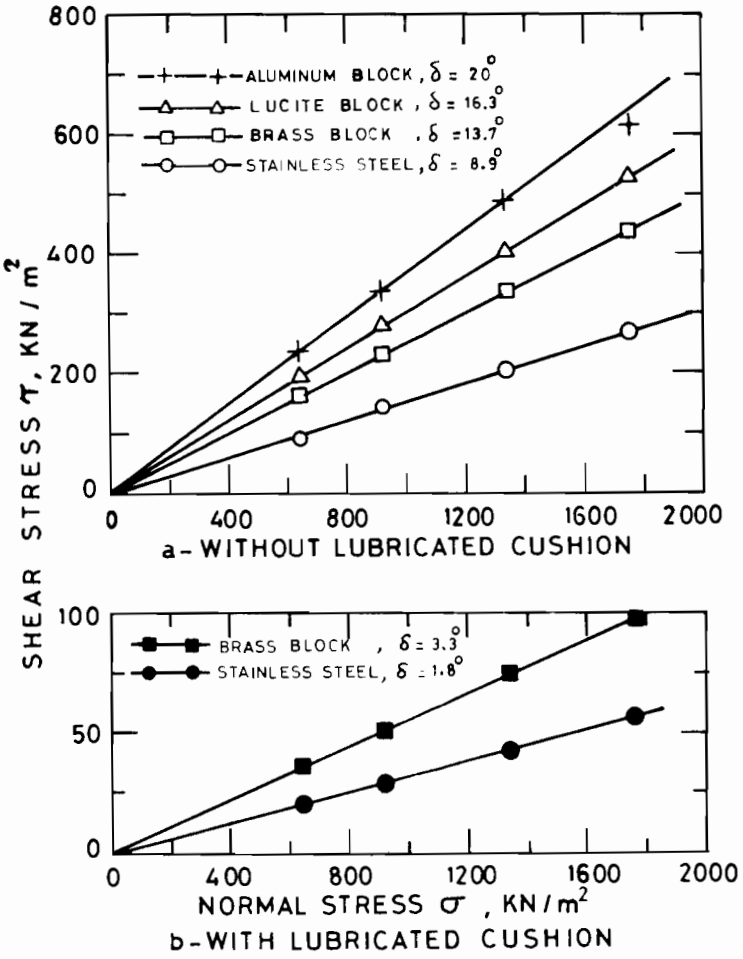

Fig. 3. Results of friction tests between crushed basalt and different platens materials.

steel block. Consequently, polished stainless steel was used for the design of the platens.

The effects of lubricated cushion thickness and particle size on the end restraint of triaxial specimens subject to compression have previously been studied (Lee 1978; Norris 1981), and results show that the end restraint decreases with increasing lubricated cushion thickness and increases with the increase of the average grain size. It has been suggested (Norris 1981) that there is an optimal thickness of cushion where the end restraint can be negligible. This optimal thickness varies with the test conditions but, for practical purposes, can be considered equal to one and one half the mean particle diameter of the material being tested. The effects of particle size and thickness of cushion on the end restraint require further study.

The preceding review suggests several trends that might be expected to play a role in drained triaxial testing using regular and lubricated platens. Thus, actual tests are needed to verify those trends applicable to low stress levels and to see if they are also

relevant to triaxial testing at high stress levels. With this in mind, a comparative test program was performed on crushed rock using regular and low-friction platens.

TEST EQUIPMENT AND INSTRUMENTATION

The triaxial apparatus used in this investigation is capable of testing cylindrical specimens about 71 mm in diameter and 178 mm long, and has the capability of using either frictionless or regular end platens. The upper regular platen, shown in Fig. 4, is made of a brass plate 25·4 mm thick and 71 mm in diameter, with a central spherical

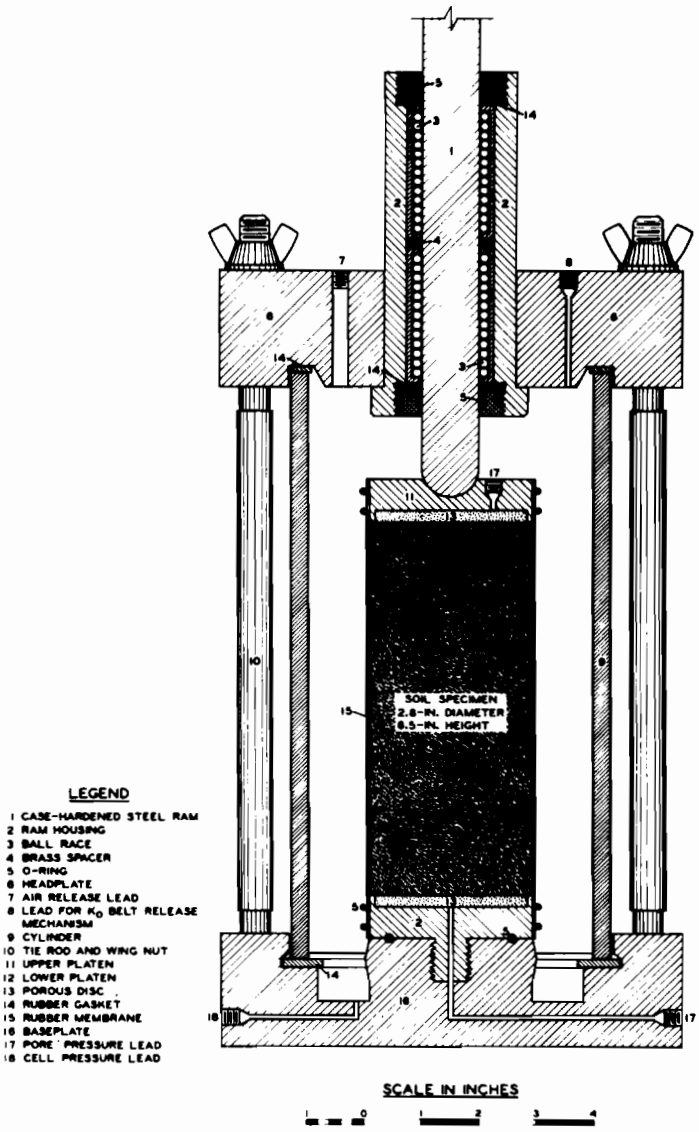

Fig. 4. Triaxial apparatus with regular platens.

seating in its upper surface to receive the loading ram. The lower surface of the platen is provided with a rough porous bronze disk, 6·4 mm thick and 68·7 mm in diameter, for drainage purposes. The lower regular platen is made similar to the upper platen and provided with a threaded end which fits the base of the apparatus. The specimen and the platens are encased in a flexible and impervious rubber membrane about 0·63 mm thick, and sealed against the platens by rubber O-rings. For higher confining pressures, a thick membrane of about 1·27 mm thickness was used. The pressure chamber, shown in Fig. 4, consists of a base, a cap, and a cylindrical shell. The base is a rigid aluminium plate provided with three leads connecting the inside instrumentation with the outside measuring devices. The first lead is used for filling the chamber with fluid which could be pressurised by an external pressure supply. The second lead is connected to the bottom of the specimen and serves to allow a free passage of pore fluid between the soil specimen and the volume measuring device. The third lead is used to connect the strain gauges mounted on the K_0 belt to the outside power supply. The cylindrical shell, 8 mm thick and having a 133 mm inside diameter, is made of aluminium and can sustain very high pressure. The cap is made of aluminium casting, with its central portion fitted tightly to reduce friction around the loading ram during the test. The loading ram, made of 19 mm diameter case hardened steel, slides through the ball race bushing and rests smoothly in the spherical depression of the upper platen. Two 9·5 mm threaded holes were made in the cap; the first is used to fit an air-release valve, and the second for the fitting which contains a piano wire used to unlock the K_0 belt. The pressure chamber is held together by three 12·7 mm-diameter stainless steel threaded rods and provided with washers and wing nuts, as shown in Fig. 4.

SPECIMEN-FORMING JACKET FOR LOW-FRICTION PLATENS

Since low-friction platens are made larger in diameter than the specimen, an ordinary forming jacket could not be used. Thus a new brass forming jacket was designed for this investigation. This jacket consists of two identical halves which form a split mold to enclose the rubber membrane stretched around the lower platen, as shown in Fig. 5. It was found that a perfect contact could not be maintained between the rubber membrane and the lower platen unless the forming jacket is pushed down against the platen. This is accomplished by using a sealing ring which consists of an annular aluminium disk open at one end so that it slides easily around the forming jacket. The sealing ring is provided with three 12·7 mm-diameter short bolts which can be connected to the base of the triaxial cell. Tightening these bolts maintains a perfect contact betwen the rubber membrane and the platen. The forming jacket and the sealing ring are illustrated in Fig. 5.

LOADING AND VOLUME-MEASUREMENT SYSTEM

The axial load is applied to the specimen by using a constant-strain testing machine. The total change in the length of the specimen caused by the applied load is measured by a dial gauge. Compressed air stored in large steel bottles is used for providing the confining pressure. A typical layout of the air pressure supply is illustrated in Fig. 6.

The volume-change measuring device, as shown in Fig. 6, consists of a 50 cm^3 Pyrex glass burette graduated to the nearest 0·1 cm^3. The top of the burette is connected to the air supply, the pressure of which can be regulated according to the magnitude of the

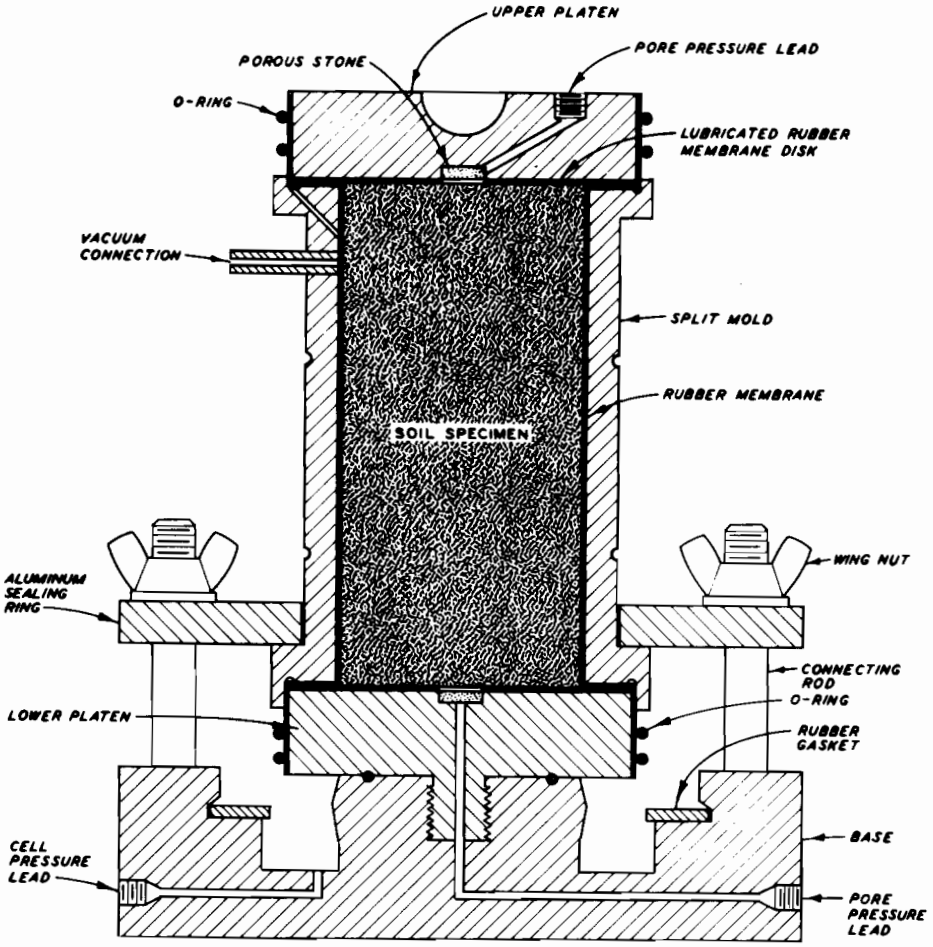

Fig. 5. Specimen forming jacket with sealing ring.

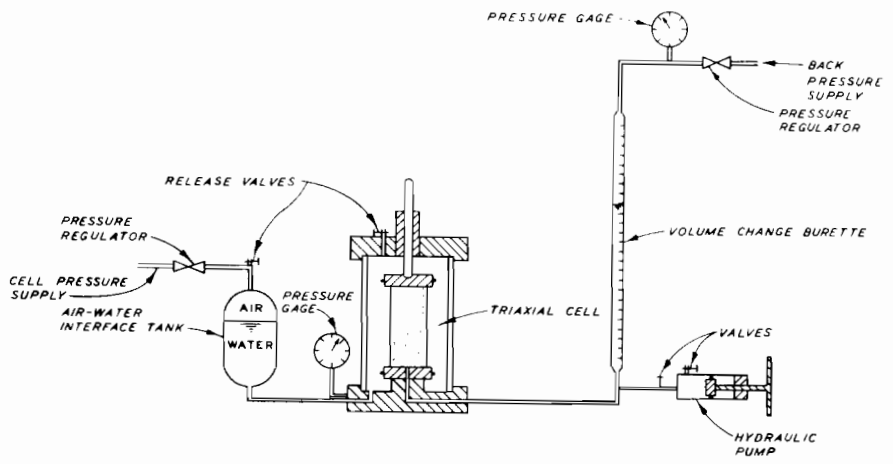

Fig. 6. General layout of the hydraulic system.

back pressure desired during the test. The bottom of the burette leads to a tube ending with a union tee. One branch of the tee is connected to a water pump to adjust the level of water before the test.

K_0 BELT

The K_0 belt is made of a thin brass alloy band welded to a short piece of hose clamp with an adjusting thumb screw. The two ends of the belt and a small pin form a hinge which can be locked and disengaged very easily. Four strain gauges are mounted on the brass band, with two dummy gauges placed along the vertical axis on the portion of the foil band which projects above and below the main band. Fig. 7 shows the components of the K_0 belt and the release mechanism. At the beginning of the K_0 consolidation stage, the thumb screw is loosened and the pin placed in position to engage the two ends of the

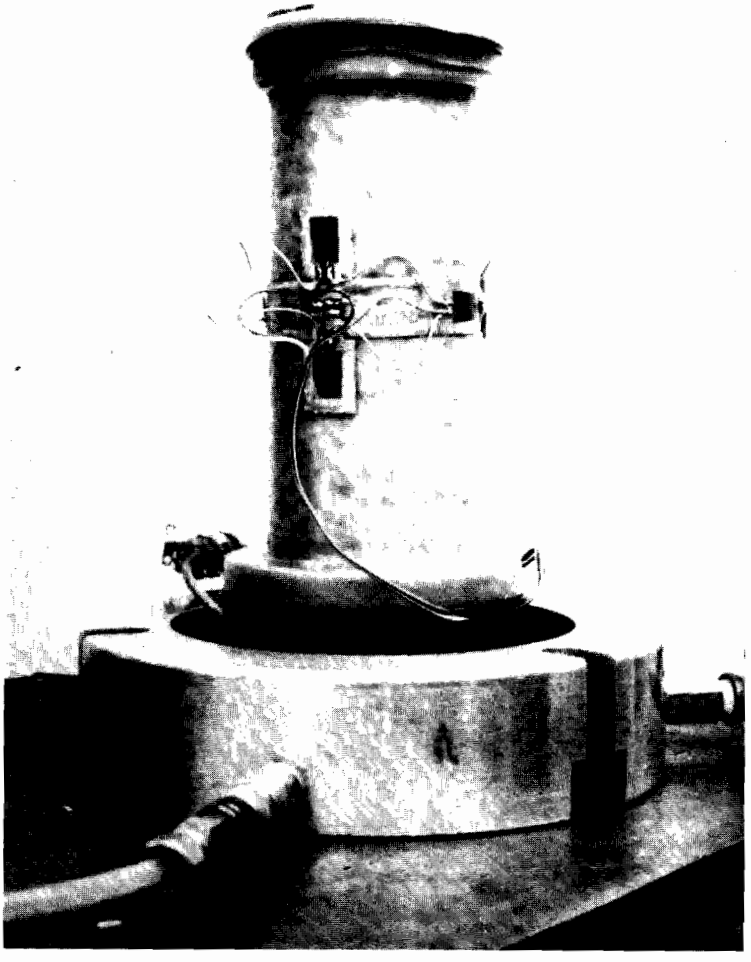

Fig. 7. K_0 belt mounted on the triaxial specimen.

belt. The thumb screw is then tightened snugly around the specimen and the pin hooked to the wire descending from the pressure chamber cup. At the end of K_0 consolidation, the wire is pulled up from outside the chamber, which removes the pin from the hinge and allows the K_0 belt to fall away from the specimen.

MATERIAL AND TESTING METHOD

The material used in the investigation was crushed basalt which consisted of highly angular particles with elongated and thin fragments. Photographs of the different fractions of the material used are shown in Fig. 8. The mineral components of the crushed basalt as identified by X-ray diffraction, are plagioclase, diopside, augite, and traces of montmorillonoid clay minerals. A summary of the physical properties of the material as obtained by the ASTM standard, is given below:

Specific gravity	2·9
Maximum void ratio	0·958

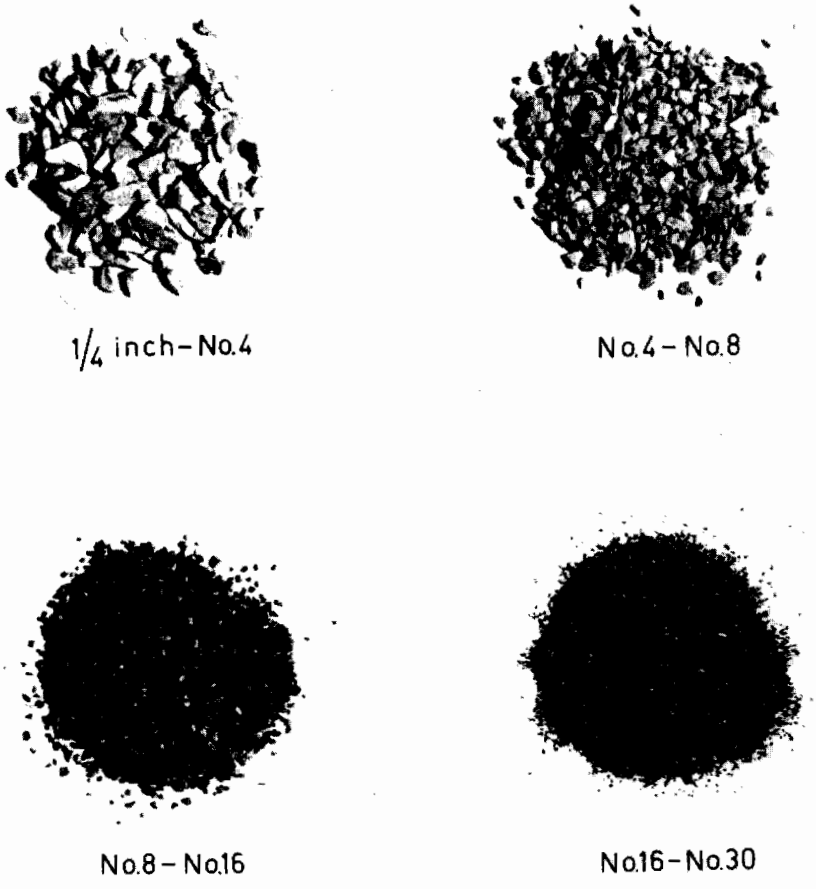

Fig. 8. Fractions of materials composing the crushed basalt.

Minimum void ratio	0·535
Coefficient of uniformity	3·31
Unconfined compressive strength of intact rock	172 MN/m^2.

The different sizes of the crushed basalt were measured accurately and mixed thoroughly to form a straight line grain size distribution curve extending from 6·3 mm to No. 30 U.S. standard sieve. The saturation procedure used consisted of flooding and boiling the mixture for about 10 min to get rid of air bubbles from the crushed rock pores, and cooling the mixture to room temperature before preparing the test specimen which is built under water.

PREPARATION OF SPECIMEN WITH FRICTIONLESS PLATENS

It was found during the early stages of the test program that more uniform radial deformation could be achieved by using a double layer of 0·63 mm greased rubber membrane below the upper platen instead of one layer. This is lower than the criteria suggested by Norris (1981) for the optimal thickness of a lubricated membrane. The lower platen was secured to the base with the rubber membrane stretched around it, and the split specimen-forming jacket was assembled to form the mold. The sealing ring was placed around the forming jacket, and the bolts were tightened to the base in order to force the specimen-forming jacket against the lower platen. Finally, the excess rubber membrane was rolled back over the upper end of the forming jacket, and vacuum was applied so that the rubber membrane was held tightly against the inside of the specimen-forming jacket before placing the material. Water was allowed to flow from the volume-change measuring device through the porous stone into the mold in order to free any air bubbles that might be trapped in the system. The boiled crushed basalt was placed under water inside the mold in about 13 mm thick uniform layers, and each layer was compacted to obtain the desired relative density. A relative density of 100% was obtained by vigorously vibrating each layer of the material using a small hand vibrator, while a relative density of 70% was obtained with a gentle vibration of the cell base after placing all material in the mold. Once the material was completely placed in the mold, the surface was levelled off and the top platen was placed in its proper position. The rubber membrane was then rolled back to the platen, and two O-ring seals were placed around it to prevent leakage. Finally, 20 KN/m^2 vacuum was applied to the specimen to make it self-supporting and the specimen former was disassembled from around the specimen. Several readings of the height and diameter of the specimen were recorded for density, stresses and strains computation.

For confining pressures of 413 and 861 KN/m^2, only one membrane was used. For a confining pressure of 2067 KN/m^2 a second rubber membrane, 0·6 mm thick, was placed over the specimen to protect it in case the material penetrated the first membrane during the test. For a lateral pressure of 3445 KN/m^2, strips of teflon 30 mm wide, 80 mm long, and 0·4 mm thick with overlaps of about 6·3 mm were placed around the first membrane and then another membrane, 0·3 mm thick, was carefully placed around the specimen. When it was desired to consolidate the specimen under K_0 conditions, the K_0 belt was secured in position before assembling the triaxial chamber around the sample. Finally, the components of the triaxial apparatus were assembled around the specimen; the loading ram was brought in contact with the top platen, and

the confining fluid was allowed to fill the pressure chamber. Vacuum inside the specimen was decreased as the chamber pressure was increased by the same amount to maintain constant effective stress. At the end, the chamber pressure was 20 KN/m^2 while the pore pressure was atmospheric. A high degree of saturation was obtained by applying 140 KN/m^2 back pressure.

ISOTROPICALLY CONSOLIDATED TEST DATA

Three series of tests were conducted throughout this program. In the first series, the material was consolidated isotropically and rough end platens were used in the test. In the second series, the material was also consolidated isotropically, but enlarged low-friction end platens were employed. Specimens of the third series were consolidated anisotropically (i.e. K_0 consolidation) with low-friction end platens. All specimens were prepared at two initial relative densities, 70 and 100%. The maximum consolidation pressures used in the test program were 413, 861, 2067 and 3445 KN/m^2. The methods of consolidation can be summarised as follows: After the completion of the isotropic consolidation phase, all specimens were sheared under drained conditions at a constant rate of strain. A summary of tests, using regular and low-friction platens, is presented in Tables 1 and 2. Each test was terminated when the applied axial load started to decline or when it stopped increasing during the increase of axial deformation.

ANISOTROPIC CONSOLIDATION TEST DATA

K_0 consolidation was performed by increasing the cell pressure and the axial load simultaneously by small increments such that the diameter of the specimen using the K_0

Table 1. Isotropically consolidated drained triaxial tests with regular platens

Test no.	End of consolidation		Peak stress difference, $(\sigma_1-\sigma_3)f$					Initial tangent modulus
	σ_3' (MN/m^2)	Dr (%)	σ_3' (MN/m^2)	σ_1 (MN/m^2)	ϕ' (Deg.)	ε_1 (%)	$\Delta V/V$ (%)	E_i, MN/m^2
1	0·413	72·2	0·413	2·612	46·63	11·2	−1·84	75·79
2	0·413	71·5	0·413	2·609	46·60	12·7	−1·79	75·71
3	0·861	69·5	0·861	4·917	44·59	17·1	−5·59	103·45
4	0·861	71·2	0·861	4·814	44·15	16·3	−5·61	105·07
5	2·067	70·0	2·067	10·589	42·31	23·3	−12·06	158·47
6	2·067	68·7	2·067	10·386	41·92	21·7	−11·83	141·25
7	3·445	73·7	3·445	16·595	41·01	26·5	−14·16	192·97
8	3·445	69·3	3·445	16·307	41·63	27·8	−15·26	189·47
9	0·413	97·6	0·413	2·887	48·56	9·1	−0·05	117·13
10	0·413	97·6	0·413	2·921	48·78	9·7	+0·19	96·46
11	0·861	97·9	0·861	5·308	46·13	12·8	−2·64	151·58
12	0·861	99·8	0·861	5·311	46·14	11·2	−2·60	175·69
13	2·067	97·9	2·067	11·070	43·26	19·2	−7·77	196·36
14	2·067	100·0	2·067	11·267	43·63	18·8	−7·93	213·59
15	3·445	99·8	3·445	17·085	41·64	20·2	−10·37	261·82
16	3·445	97·4	3·445	17·001	41·53	19·5	−11·00	258·37

Table 2. Isotropically consolidated drained triaxial tests with low-friction platens

Test no.	End of consolidation		Peak stress difference, $(\sigma_1-\sigma_3)f$					Initial tangent modulus
	σ_3' (MN/m^2)	Dr (%)	σ_3' (MN/m^2)	σ_1 (MN/m^2)	ϕ' (Deg.)	ε_1 (%)	$\Delta V/V$ (%)	E_i, MN/m^2
17	0·413	73·3	0·413	2·230	43·4	11·5	−0·81	72·34
18	0·413	71·3	0·413	2·163	42·8	15·5	−1·54	68·90
19	0·861	70·4	0·861	4·083	40·7	20·4	−5·13	89·57
20	0·861	71·4	0·861	4·094	40·7	21·8	−5·44	99·90
21	2·067	70·5	2·067	8·838	38·4	27·0	−11·95	137·80
22	2·067	71·6	2·067	8·810	38·3	25·1	−11·29	142·97
23	3·445	70·0	3·445	14·518	38·1	28·3	−13·44	172·25
24	3·445	69·5	3·445	14·320	37·7	28·9	−14·87	171·29
25	0·413	97·3	0·413	2·530	46·0	11·8	+1·19	95·08
26	0·413	99·7	0·413	2·541	46·0	11·7	+0·75	96·46
27	0·861	95·7	0·861	4·579	43·1	18·1	−2·45	134·36
28	0·861	99·6	0·861	4·674	43·5	19·5	−1·67	148·13
29	2·067	100	2·067	9·334	39·6	22·9	−7·69	206·70
30	2·067	100	2·067	9·432	39·8	23·6	−7·98	189·47
31	3·445	100	3·445	15·002	38·8	25·4	−10·28	254·93
32	3·445	100	3·445	15·152	39·0	26·2	−10·83	234·26

belt was kept constant. The relationship between σ_1' and σ_3', for the crushed basalt tested at medium and high relative densities, is presented in Fig. 9. The slope of these curves at any point is equal to K_0. Unlike isotropic consolidation, K_0 consolidation permits the application of the desired confining pressure without causing any radial deformation in the specimen, thus eliminating the influence of end restraint. In addition, the area of the specimen at the end of consolidation is not affected by the membrane penetration while that for isotropically consolidated specimens requires correction due to this penetration. In this study, all volume-change measurements

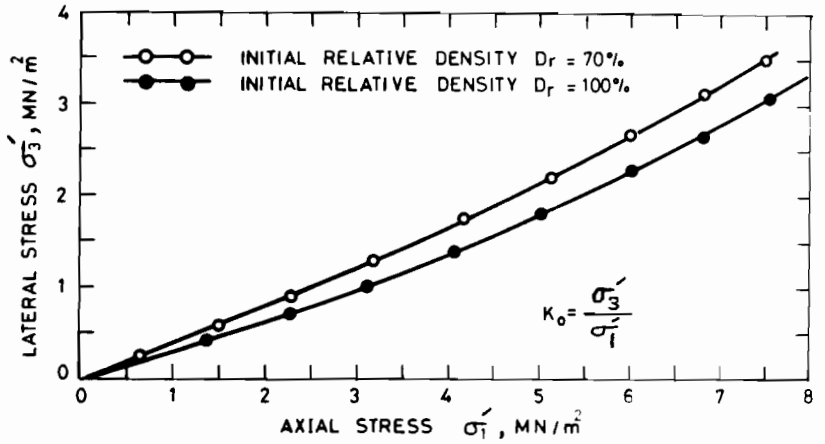

Fig. 9. Relationship between σ_3' and σ_1' during K_0 consolidation.

during isotropic consolidation were corrected for membrane penetration using the procedure presented in Appendix A.

All the K_0 consolidated specimens were sheared under drained conditions at a constant rate of strain. The stress–strain and volume-change relationships for specimens consolidated under K_0 conditions and sheared using low-friction platens are presented in Fig. 10.

DISCUSSION OF RESULTS

In this investigation, the length:diameter ratio was kept slightly more than 2 for specimens tested using low-friction platens to provide a better comparison with data obtained from conventional triaxial testing. Since crushed basalt is very pervious, drainage was only provided at the bottom of the specimen. The finite element analysis (Fig. 2) shows that, for restrained ends, a significant amount of shear stress develops at the specimen ends but the intensity of the stress decreases quickly in moving towards the centre of the specimen. This high concentration of shear stress near the ends of the

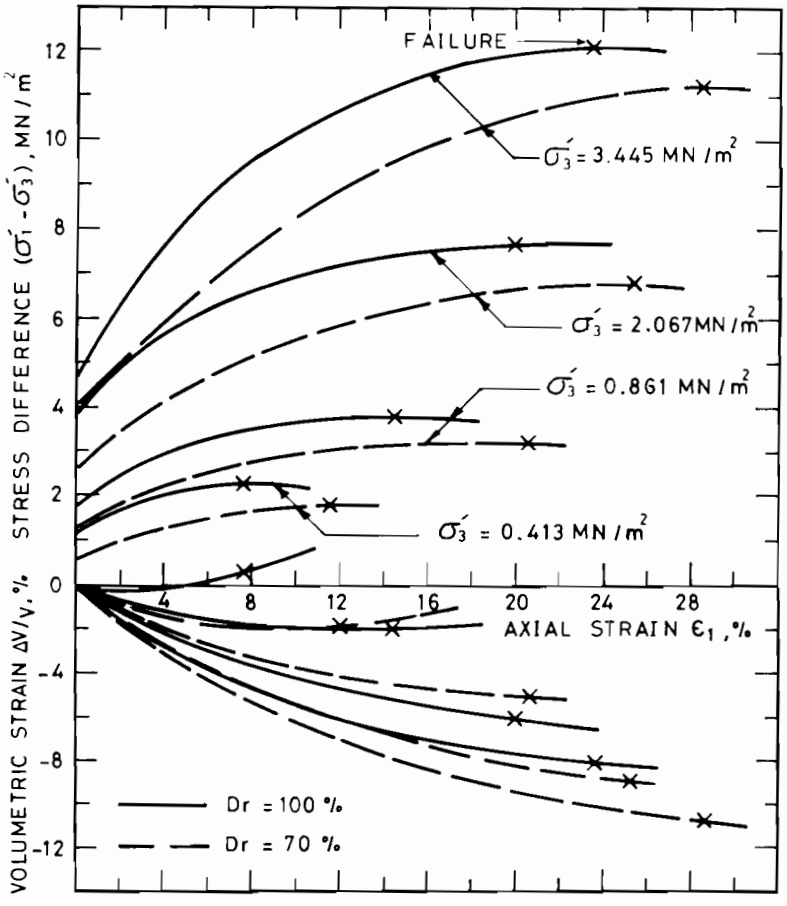

Fig. 10. Stress–strain and volume-change relationships during shear for K_0 consolidated specimens.

regular platens inhibits the development of radial deformations throughout the specimen and causes bulging in its middle section. For truly frictionless platens the shear stress would be equal to zero throughout the entire specimen, and the specimen would deform as a right cylinder. This has been confirmed repeatedly by actual tests as indicated in Fig. 11, which shows that lubricated end platens improve significantly the uniformity of radial deformation around the tested specimens. While a specimen with regular end platens deformed in the typical barrel shape during shear, the one with lubricated platens deformed almost as a right cylinder. Test results also show that specimens consolidated under K_0 condition exhibit a much more uniform deformation distribution during shear than those consolidated isotropically, especially at high stress levels.

COMPARISON OF STRESS–STRAIN RELATIONS

The results of this investigation indicate that the stress–strain relationship during shear is linear at the early part of the test then starts to curve with increasing strain until failure. It was considered that the material reached failure when the stress difference $(\sigma_1-\sigma_3)$ reached its maximum value on the stress–strain plot. The slope of the initial straight line portion of the stress–strain graph is equal to the initial tangent modulus E_i. The values E_i presented in Tables 1 and 2 were plotted against σ_3' on a logarithmic scale as shown in Fig. 12. Each point on the plot represents the average of two similar tests. It is clear from the figure that tests with regular platens exhibit higher initial tangent moduli (about 10% higher) than those obtained with low-friction platens.

Based on the experimental data presented in Fig. 12, the best-fit equation relating the initial tangent modulus to the confining pressure σ_3' and the initial relative density, Dr, using the low-friction platens, can be expressed as

$$E_i = K\,(\mathrm{Dr})\,P_a\left(\frac{\sigma_3'}{P_a}\right)^n \qquad (1)$$

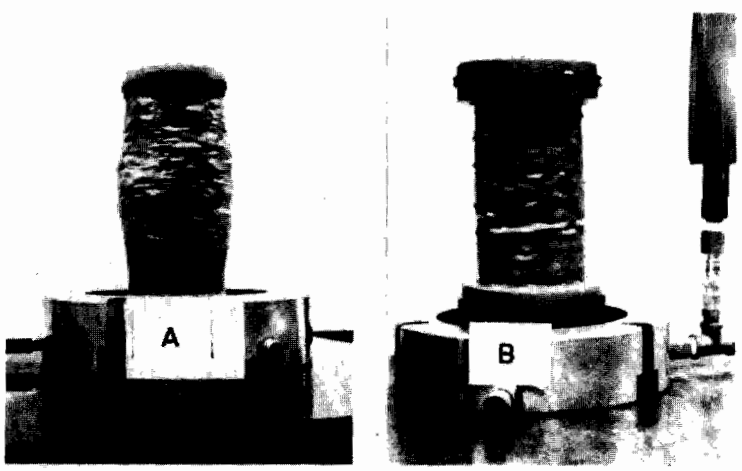

Fig. 11. Influence of end restraint on the radial deformation in triaxial compression.

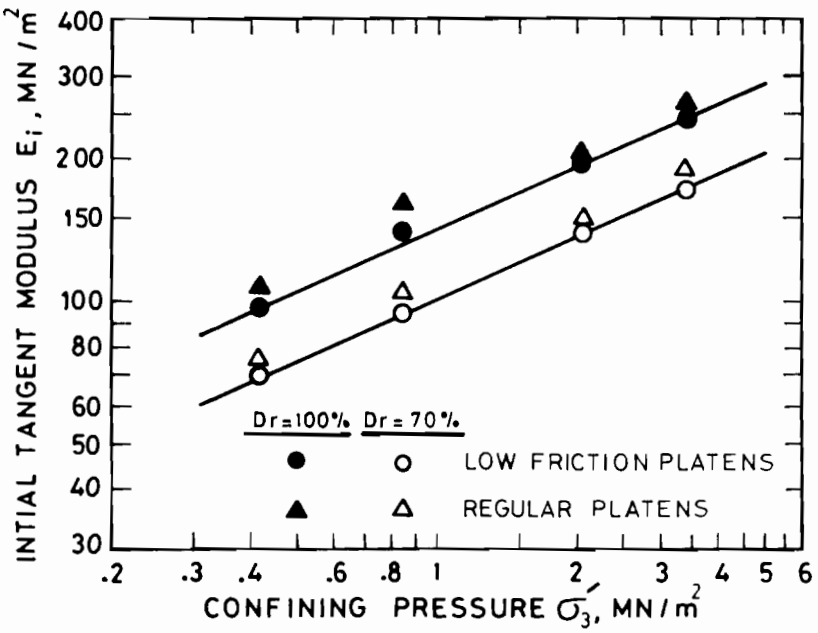

Fig. 12. Relationships between E_i and σ_3'.

where P_a is the atmospheric pressure equal to 101·3 KN/m^2, Dr is the relative density in percent, n and K are parameters. For the range of data collected in this study, it is found that $n=0{\cdot}43$ and $K=5{\cdot}4$.

The variation of volumetric strains with respect to axial strains during shear for K_0 consolidated specimens is presented in Fig. 10. It is clear that the variation is highly non-linear. The isotropically consolidated specimens show a similar non-linear behaviour, but exhibit a more compressional volumetric strain than those consolidated under K_0 condition. Lubricated low-friction end platens in general cause the crushed basalt to produce the slightly less compressional volumetric strain in comparison with the tests using regular platens. One important parameter which provides a measure for compressibility of the material and reflects to a certain extent its undrained strength is the volumetric strain at failure, $(\Delta V/V)f$. Variation of the volumetric strain at failure with respect to the effective confining pressure, σ_3' for the isotropically consolidated tests is presented in Fig. 13. Each point in this figure represents the average of two similar tests. It is clear that lubricated ends tend to produce less compressional volumetric strain at failure than when using regular platens. However, the difference is so small that it can be considered insignificant for practical purposes. A similar trend was observed with fine sand (Lee 1978; Norris 1981).

In this study, the axial strain which the material exhibits at maximum stress difference, $(\sigma_1-\sigma_3)$, is considered to be equal to the failure strains. Values of failure strains for the isotropically consolidated crushed basalt are presented in Tables 1 and 2. Average values of failure strains were plotted against the confining pressure, σ_3, and the results are presented in Fig. 14. This figure shows that the failure strain for both types of platens increased rapidly with σ_3 until the effective confining pressure reached a certain value beyond which the increase in σ_3 would have little effect on the failure

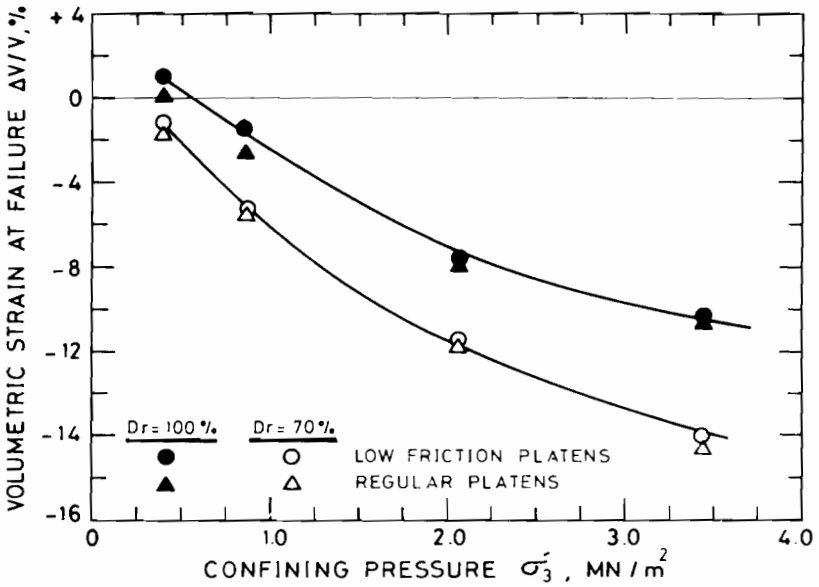

Fig. 13. Relationships between volumetric strain at failure and σ_3'.

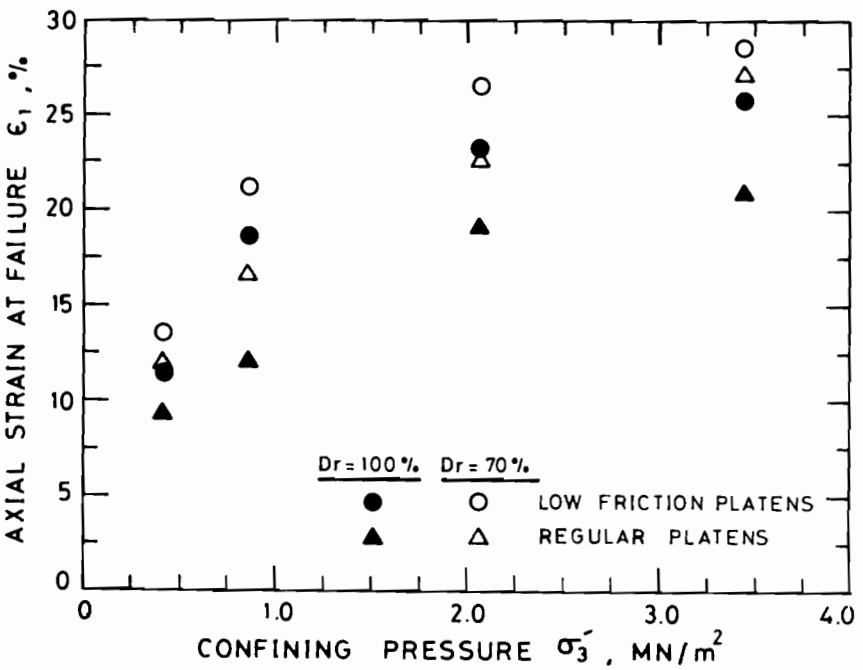

Fig. 14. Variation of axial strain at failure and σ_3'.

strain. As far as the end restraint is concerned, Fig. 14 clearly shows that low-friction platens cause the triaxial specimens to exhibit much more axial strain at failure than regular platens do.

COMPARISON OF STRENGTH

The angle of internal friction, ϕ' as calculated by Mohr–Coulomb equation was used to measure the strength of the crushed basalt. Summary of ϕ' for the isotropically consolidated crushed basalt is presented in Tables 1 and 2 for tests using regular and low-friction platens respectively. The variation of ϕ' with respect to effective confining pressure, σ_3, is presented in Fig. 15. Every point in this figure represents the average of two similar tests. For both types of end conditions the angle of internal friction decreases at a decreasing rate with increasing confining pressure. Tests with regular end platens showed a significantly higher strength than comparable tests using low friction platens. The difference between the two types of tests, as depicted in Fig. 15 is about 3° for the low confining pressure and about 2° for high confining pressure. A similar conclusion was obtained previously on testing sands (Norris 1981; Lee 1978; Rowe & Barden 1964). Values of ϕ' for K_0 consolidated tests were similar to those obtained from isotropically consolidated tests using low-friction platens. This confirms that the method of consolidation has no significant effect on the drained angle of internal friction, ϕ'.

Grain size distribution curves before testing and after shear indicated that the degree of end restraint as well as the relative density have no significant influence on the crushing of particles. However, the confining pressure appeared to be the only significant factor which contributes to particle crushing during shear.

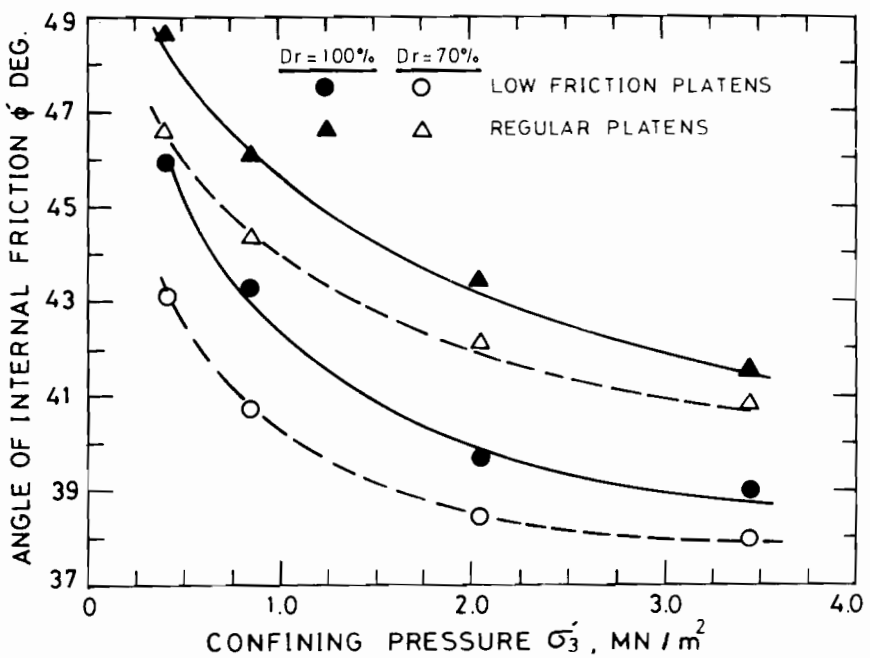

Fig. 15. Variation of ϕ' with respect to the effective confining pressure σ_3'.

CONCLUSIONS

Within the scope of the experimental investigation of this study it was found that tests with enlarged low-friction platens exhibited much more uniform boundary deformations, about 10% lower initial tangent modulus values and a larger axial strain at failure than comparable tests with regular rough platens. The results of the crushed basalt test indicate that the volumetric strain at failure is not influenced by the difference in triaxial test end conditions.

The drained strength of granular material is directly related to the angle of internal friction, ϕ'. For the crushed basalt tested, the value of ϕ' is significantly influenced by the degree of end restraint. The angle of internal friction using regular platens was about 3° more than those in comparable tests using enlarged low-friction platens, and such a difference did not significantly change with the relative density of the material or the confining pressure.

REFERENCES

Al-Hussaini, M. 1970. The influence of end restraint and method of consolidation on the drained triaxial compressive strength of crushed Napa basalt. USAE Waterways Exp. Station, MPS-70-18, Vicksburg, MS, U.S.A.

Balla, A. 1960. Stress condition in triaxial compression. J. Soil Mech. Found. Div. ASCE **86,** SM6: 57–84.

Barden, L. & McDermott, J.W. 1965. The use of free ends in triaxial testing of clays. J. Soil Mech. Found. Div. ASCE **91,** SM6: 1–24.

Bishop, A.W. & Green, G.E. 1965. The influence of end restraint on the compression strength of a cohesionless soil. Geotechnique **15** (3): 243–65.

Brady, B.T. 1971a. The effect of confining pressure on the elastic stress distribution in a radially end-constrained circular cylinder. J. Rock Mech. and Mining Science **8** (2): 153–64.

Brady, B.T. 1971b. An exact solution to the radially end-constrained circular cylinder under triaxial loading. J. Rock Mech. and Mining Science **8** (2): 165–78.

Cooling, L.F. & Golder, H.Q. 1940. Portable apparatus for compression test on clay soils. Engineering **149:** 57–58.

D'Appolonia, E. & Newmark, N.M. 1951. A method for solution of the restraint cylinder under triaxial compression. First U.S. National Conf. Applied Mech. ASME, 217–26.

Duncan, J.M. & Dunlop, P. 1968. The significance of cap and base restraint. J. Soil Mech. Found. Div. ASCE **94,** SMI: 271–90.

Filon, L.N.G. 1962. The elastic equilibrium of circular cylinder under practical system of load. Phil. Trans. Roy. Soc. London **198:** 147–233.

Girijavallabhan, C.V. 1970. Stresses in restrained cylinder under triaxial compression. J. Soil Mech. Found. Div. ASCE **96,** SM2: 783–7.

Girijavallabhan, C.V. & Mehta, K.C. 1969. Stress–strain relationship from compression test on nonlinear materials. Symposium, Application FEM in Civil Eng., Vanderbilt University, 457–80.

Lee, K.L. 1978. End restraint effects on undrained static triaxial strength of sand. J. Geotechnical Eng. Div. ASCE **104,** GT6: 687–701.

McMurdie, J.L. & Day, P.R. 1958. Compression of soil by isotropic stress. Soil Sci. Soc. Am. **22:** 18–21.

Norris, G.M. 1981. Effect of end membrane thickness on the strength of frictionless cap and base. Symposium on Laboratory Shear Strength of Soil, ASTM, STP **740:** 303–14.

Peng, S.D. 1971. Stresses within elastic circular cylinders loaded uniaxially and triaxially. J. Rock Mech. and Mining Science **8** (5): 147–233.

Perloff, W.H. & Pombo, L.E. 1969. End restraint effects in the triaxial test. Seventh Internat. Conf. SMFE, Mexico.

Pickett, G. 1944. Application of Fourier method to the solution of certain boundary value problems in the theory of elasticity. J. App. Mech. ASME **2:** 176–82.

Radhakrishnan, N. 1972. Analysis of triaxial tests by the finite element method. WES Symposium on Application of the Finite Element Method in Geotechnique, pp. 947–99.

Roscoe, K.H., Schofield, A.N. & Thurairajah, A. 1964. An evaluation of test data for selecting a yield criteria for soils. ASTM, STP **361:** 111–28.

Rowe, P.W. & Barden, L. 1964. Importance of free ends in triaxial testing. J. Soil Mech. Found. Div. ASCE, **90** SMI: 1–27.

Shockley, W.G. & Ahlvin, R.G. 1960. Nonuniform conditions in triaxial test specimens. ASCE Conf. on Shear Strength of Cohesive Soil, pp. 341–57.

(Received 6 September 1983, revised 14 November 1983)

APPENDIX A: MEMBRANE PENETRATION

The apparent volume change of the specimen as measured by the volume-change device during consolidation is composed of two components: one due to densification of the material and the other is due to membrane penetration. Unless the volume change due to the membrane is known, stress measurements which are based on the actual volume change of the specimen will be in error.

The method suggested for evaluating membrane penetration is based on the measurement of the actual volume change, from strain measurements of the specimen, and the apparent volume-change measurements obtained from the water collected by the volume-change device. The difference between the two volume changes is equal to the volume change due to membrane penetration.

Calculation of membrane penetration for crushed basalt is based on the assumption that soil under isotropic state of stress behaves as elastic material

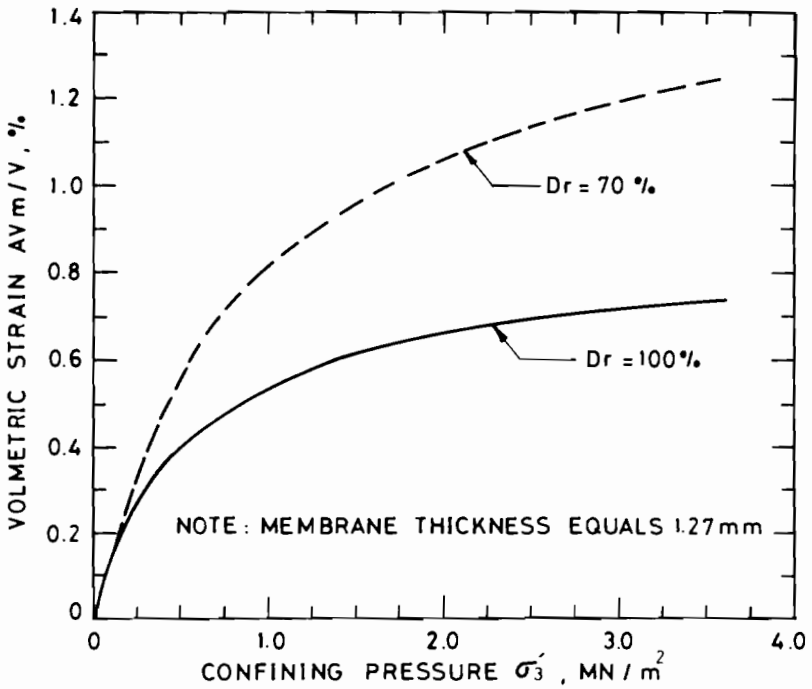

Fig. A1. Relationship between volume of membrane penetration and cell pressure.

(McMurdie & Day 1958; Roscoe *et al.* 1964) whose volumetric strain is equal to three times the axial strain, Thus, from the knowledge of volumetric strain and the initial volume of the specimen, the actual volume change under isotropic compression can be calculated. The difference between the volume change measured by the burette and that which is calculated from the assumption of elasticity is the volume change due to membrane penetration. The error in volumetric strain due to membrane penetration for the crushed basalt tested is presented in Fig. A1.

تأثير تقييد النهايات في الفحوص ثلاثية المحاور على مقاومة البازلت المكسر

مساعد الحسيني
كلية الهندسة والبترول بجامعة الكويت

خلاصة

هذا البحث هو وصف لنتائج عدة تجارب أجريت على البازلت المكسر في جهاز الضغط ثلاثي المحاور لمعرفة تأثير تقييد النهايات وضغوط الاندماج على الاجهاد والانفعال وعلى متانة المادة . استعمل في هذا البحث الجهاز التقليدي ثلاثي المحاور وكذلك جهاز مشابه يحتوي على غطاء عينة موسعة معدومة الاحتكاك .

استحضرت جميع العينات بكثافتين نسبيتين (٧٠٪ و ١٠٠٪) ومن ثم سلط عليها اجهاد القص مع السماح بنزح كامل للماء من العينات بعد ان سلط عليها ضغوط اندماج مقدارها ٤١٣ و ٨٦١ و ٢٠٦٧ و ٣٤٤٥ كيلونيوتن/م^2 .

أظهرت النتائج ان تقليل الاحتكاك على نهايات العينة أثناء التجربة يساعد على توزيع الانفعال القطري والعمودي بصورة متجانسة في العينة . كما ان تقليل الاحتكاك حول نهايات العينة ليس له تأثير على التغيير الحجمي للمادة ولكنه يؤدي إلى تقليل زاوية الاحتكاك الداخلي لها بالمقارنة إلى عينة مشابهة فحصت بالجهاز ثلاثي المحاور التقليدي .